Brian T. Phelan, originally from Downers Grove, IL, is a senior at the University of Illinois, Urbana-Champaign. After obtaining his Bachelor's in Chemistry, he plans to pursue a Master's in Teaching Chemistry at the University of Illinois. During the summer of 2008 he was a Pre-Service Teacher intern at Argonne National Laboratory (ANL). Brian is a member of the American Chemical Society. In his spare time, he enjoys Ultimate Frisbee and skiing.

Deborah J. Myers is the leader of the Hydrogen and Fuel Cell Materials group in Argonne National Laboratory's Chemical Sciences and Engineering Division. She received her Ph.D. in Analytical Chemistry from the University of Illinois, Urbana-Champaign, specializing in Physical Electrochemistry. She joined ANL Aqueous Corrosion group in 1989 where she studied the kinetics of several corrosion-related processes and the oxidation-reduction of platinum using in-situ X-ray reflectivity. Dr. Myers joined Argonne's Fuel Cell Department in 1993, where she has worked on a variety of fuel cell and hydrogen-related projects. These projects include materials development and characterization for solid oxide, direct methanol and polymer electrolyte fuel cells, hydrocarbon fuel processing catalysts and solid oxide electrolysis cells. Her current projects include in-situ X-ray absorption and scattering studies of Pt-based fuel cell catalyst degradation, X-ray absorption studies of base metal electrocatalysts and the development of non-platinum bimetallic polymer electrolyte fuel cell catalysts.

Matt C. Smith is a postdoctoral student at Argonne National Laboratory. He received his Ph.D. from the University of East Anglia, UK, in 2002 for a study synthesizing structural and functional bio-inspired models of the active sites of nickel based metalloproteins responsible for hydrogen and carbon monoxide/dioxide catalysis. He worked as a postdoctoral student at the University of California–Davis studying the same metalloproteins, and other iron-sulfur proteins such as nitrogenase, using X-ray spectrocopies with an emphasis on nuclear resonance vibrational spectroscopy. Dr. Smith's current work employs X-ray techniques to examine in-situ hydrogen/oxygen catalysis in polymer electrolyte fuel cells.

Preliminary In-Situ X-Ray Absorption Fine Structure Examination of Pt/C and PtCo/C Cathode Catalysts in an Operational Polymer Electrolyte Fuel Cell

Brian T. Phelan, Deborah J. Myers and Matt C. Smith

ABSTRACT

State-of-the-art polymer electrolyte fuel cells require a conditioning period to reach optimized cell performance. There is insufficient understanding about the behavior of catalysts during this period, especially with regard to the changing environment of the cathode electrocatalyst, which is typically Pt nanoparticles supported on high surface area Vulcan XC-72 carbon (Pt/C). The purpose of this research was to record preliminary observations of the changing environment during the conditioning phase using X-Ray Absorption Fine Structure (XAFS) spectroscopy. XAFS was recorded for a Pt/C cathode at the Pt L_3-edge and a PtCo/C cathode at both the Pt L_3-edge and Co K-edge. Using precision machined graphite cell-blocks, both transmission and fluorescence data were recorded at Sector 12-BM-B of Argonne National Laboratory's Advanced Photon Source. The fluorescence and transmission edge steps allow for a working description of the changing electrocatalyst environment, especially water concentration, at the anode and cathode as functions of operating parameters. These features are discussed in the context of how future analysis may correlate with potential, current and changing apparent thickness of the membrane electrode assembly through loss of catalyst materials (anode, cathode, carbon support). Such direct knowledge of the effect of the conditioning protocol on the electrocatalyst may lead to better catalyst design. In turn, this may lead to minimizing, or even eliminating, the conditioning period.

Introduction

Polymer electrolyte fuel cells (PEFCs) are approaching commercial viability as an efficient alternative to the internal combustion engine (ICE). Hydrogen-fueled PEFCs are targeted for automotive applications due to their high efficiency and benign emissions [1]. PEFCs are currently used for stationary applications due to the less demanding conditions, such as a relatively constant load and well-controlled environment. The load in automotive applications is constantly changing, exacerbating catalyst degradation through mechanisms associated with repeated oxidation and reduction of the catalyst, and is a major issue preventing widespread fuel cell adoption [2]. Additional issues include the cost of platinum group metal (PGM) electrocatalysts (such as Pt or Pd) used in fuel cells and the conditioning phase required to reach optimal performance.

The PEFCs studied in this investigation are constructed with a proton exchange membrane (PEM) separating the anode and cathode catalysts, which in turn are sandwiched between gas diffusion layers, compression gaskets and graphite cell blocks (Figure 1). Cutting-edge electrocatalysts are nanoparticles supported on carbon which maximize the surface area of the electrocatalyst and minimize precious metal loadings, thus minimizing cost. A second technique employed to minimize the use of precious metal and

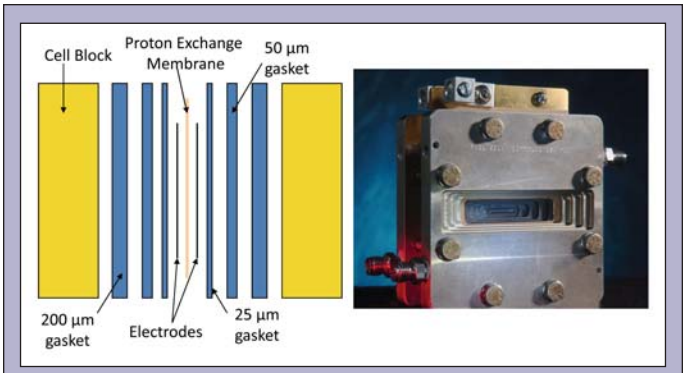

Figure 1. Schematic of the MEA and fuel cell (left) and the constructed cell (right), showing the precision machined windows through which the X-ray beam was directed.

increase durability and activity is doping the PGM with a common base metal, such as cobalt, iron or nickel [3].

State-of-the-art Pt-containing cathode electrocatalysts benefit from a conditioning phase prior to sustained operation to attain improved and stabilized performance [4]. Different protocols exist for implementing the conditioning phase. These protocols include: changes in runtime, electrical conditions, humidity levels and temperatures of the fuel cell and gases [4]. There is insufficient understanding of the conditioning phase, though it is widely accepted that the processes responsible for conditioning are either modifications of catalyst structure, humidifications of the ionomer in the electrode layer or of the membrane, or the establishing of three-phase boundaries in the electrocatalyst layers. Increased knowledge of the changes in the catalyst layers (primarily for the cathode electrocatalyst since oxygen reduction at the cathode is the kinetically limiting event in the fuel cell reaction) and of the dynamic environment within the fuel cell will improve future catalyst design and refine operational parameters, cell configuration and assembly. Ultimately this may yield designs that can minimize, or even eliminate, the time and material costs of conditioning.

X-ray Absorption Fine Structure (XAFS) spectroscopy is an ideal tool for probing PEFCs in-situ since X-ray radiation can be tuned to the energy of electronic interactions in specific atomic species [5]. In-situ spectroscopy, as opposed to traditional post mortem style ex-situ analysis, permits observation of the catalyst during the conditioning phase, allowing interpretation of changes as they occur.

Here, the focus was on Pt-based cathode electrocatalysts, including a Pt on C (Pt/C) electrocatalyst and a PtCo alloy on C (PtCo/C) electrocatalyst. XAFS was recorded at the Pt-L_3 edge for the Pt/C cathode and at the Pt-L_3 edge and Co-K edge, separately, for the PtCo/C cathode. When energies are tuned at or above the absorption edges for Pt and Co respectively, incident X-rays are absorbed by the Pt and Co atoms in the X-ray beam path. This results in excitation of an electron within the atoms and a corresponding decrease in the transmission of X-rays through the entire sample. The decrease in transmission is thus correlated with absorption of X-rays at both the anode and cathode. When the X-rays are of sufficient energy to eject electrons from a core shell of the absorbing atom, a vacancy is created which is filled by an electron from an outer shell, producing fluorescence. The fluorescence wave does not traverse through the entire cell. It only interacts with materials from the cathode and thus contains information solely pertaining to the cathode. XAFS data is manipulated mathematically to provide information of the atomic environment, typically yielding information on coordination and oxidation states of the absorbing atom and of neighboring atoms, and bond distances.

The XAFS spectra can be broken down into three portions, the pre-edge, the absorption edge (X-ray Absorption Near Edge Structure, XANES) and the post-edge (Extended X-ray Absorption Fine Structure, EXAFS). The focus of this paper is a preliminary qualitative analysis involved with the variations observed in the edge step, $\Delta\mu(E_0)$, which is the difference in height at the absorption energy, E_0, between an algorithm fitted to the pre-edge and an algorithm fitted to the post-edge (Figure 2) [6]. Correlations and disparities between the changes in edge steps between scans provide information relevant to the environment within the PEFC, especially regarding water volume at the electrodes and the quantity of mass present within the beam. A detailed directory of the possible changes in edge steps along with credible explanations for each situation can be found in Table 1. Two Pt-Pd membrane electrode assemblies (MEAs) with Pt/C and Pd/C cathode and anode electrocatalysts respectively, and two PtCo/C cathode and Pd/C anode MEAs were conditioned through stage 1 and stage 2 of a protocol recommended for cell conditioning by the United States Fuel Cell Council (USFCC) [4]. Transmission and fluorescence was recorded for each MEA throughout the conditioning phase, however several scans had to be discarded because of glitches in the spectra, large drops in signal typically due to water bubbles passing through the cell. The edge steps of the fluorescence and transmission spectra were analyzed and employed to explain the catalyst condition and cell environment during the conditioning phase.

	Fluorescence Edge Step	Transmission Edge Step
Increase	Loss of H_2O on cathode	Gain of H_2O
Decrease	Gain of H_2O, loss of Pt	Loss of H_2O, carbon support, Pt, or Pd

Table 1. Correlation of an increase or a decrease in the fluorescence or transmission edge step with fuel cell events.

Methods

Theoretical

XAFS spectra were recorded simultaneously in transmission and fluorescence geometries. The focus of this analysis is the edge step of the spectra, a value obtained by fitting one algorithm to the pre-edge and a second algorithm to the post-edge, extending both algorithms beyond the absorption edge and calculating the difference between the two lines (algorithms) (Figure 2).

The XAFS equation is given as:

$$\frac{\mathbf{I}_0}{\mathbf{I}_1} = e^{-\mu \cdot x} \quad (1)$$

where μ is the absorption coefficient of the absorbing species and x is the thickness of the material within the beamline. For the transmission spectra, I_0 represents the beam energy before encountering the cell and I_1 represents the transmission recorded. The fluorescence spectra were qualitatively analyzed under the simplified assumption that the ratio of the fluorescence detected to the original beam was proportional to the right hand side of Equation 1. The results will be represented in terms of apparent thickness, as the absorption coefficient of the absorbing species is

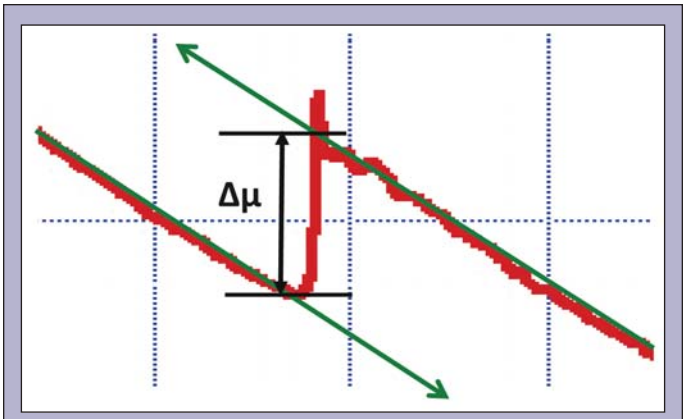

Figure 2. Edge step of a transmission spectrum. The edge step is the difference between the algorithm fitted to the pre-edge and post-edge at the absorption energy. This description can be applied to fluorescence spectra as well.

constant. This leaves any change in edge step to be caused by x, the thickness of the material within the path of the beam.

Changes in the edge step can be interpreted as meaningful observations regarding the dynamic state of the fuel cell. Fluorescence events will only portray information pertaining to the cathode as the fluorescence has a limited penetration depth. Transmission data can yield information on either the cathode or anode, allowing for the detection of differences between the events and environments on both the anode and cathode.

Experimental

XAFS spectra were recorded at Sector 12-BM-B, a bending magnet beamline, at the Advanced Photon Source at Argonne National Laboratory (ANL) using a Si(111) monochromator detuned at least 10% to reject higher harmonics. Data were acquired in transmission and fluorescence geometries using an ionization chamber, ionization chamber 1 and a liquid dinitrogen cooled 13-element Ge detector respectively. Measurements were obtained using precision machined graphite cell blocks that had windows milled down to 12 one thousandths of an inch on each side, allowing for transmission data collection. Spectra were analyzed using standard methods with the ATHENA/ARTEMIS software based on the Feff code, and referenced to pure metal standards placed downstream of the sample between ionization chamber 1 and ionization chamber 2.

This experiment looked at two different cathode electrocatalysts made by BASF E-TEK, one being 20 wt% Pt nanoparticles supported on high surface area Vulcan XC-72 carbon and the other 30 wt% PtCo nanoparticles supported on high surface area Vulcan XC-72 carbon support. The membrane electrode assembly consisted of a Nafion® 115 polymer electrolyte membrane between the two electrodes. The gasket configuration on each side was identical, a 25 µm, 50 µm and 200 µm gasket, moving away from the center. This setup was sandwiched in between precision machined graphite blocks, containing single serpentine flowfield gas flow channels. The cell was completed with gold plated electrical end blocks that were also machined to contain a window at the point of X-ray passage. The cells were constructed according to USFCC protocol [4]. The Pt-Pd MEAs consisted of a 2.25 cm x 2.25 cm electrode with 0.1 mg/cm^2 of 30 wt% Pd on the anode and 0.1 mg/cm^2 of 20 wt% Pt on the cathode. The PtCo-Pd MEAs were a binary alloy cathode containing 0.1 mg/cm^2 of 30 wt% PtCo and 0.1 mg/cm^2 of 30 wt% Pd on the anode. Pd anodes were used in this experiment to help isolate the cathode electrocatalyst as Pt anodes would have produced additional unwanted absorption in transmission, complicating the bulk signal.

All gases used were of 99.9999% purity. During initial fuel cell warm-up, prior to operation, the gas fuels were <3.65% H_2 in He (Regen gas) on the anode and reactant grade Ar on the cathode. Once the conditioning phase protocol was initiated, the gas feeds were switched to reactant grade H_2 on the anode and reactant grade air on the cathode as the source for O_2. The gas fuels were heated at two separate locations on each line, first during humidification in the humidifiers and second in-line between the humidifiers and the fuel cell. The gaseous fuel was bubbled through the humidifiers to bring it to reactant temperature, about 5 °C below the cell temperature, and to humidify the gas, as a hydrated membrane is necessary for conduction protons and carrying out the reaction. Both the anode and cathode streams were held at 100% relative humidity to maintain a sufficient hydration cell. After travelling through the humidifiers, the gas fuels flowed through heated lines to the cell. The heating of these lines was designed to maintain the temperature of the gas and prevent water condensation that is neither beneficial to X-ray spectroscopy nor to cell performance. The gaseous fuels were pumped through the cell at flow rates corresponding to a 2:1 hydrogen:oxygen stoichiometry. The cell temperature was also recorded and maintained at a steady level for the duration of the

	Pt-Pd MEA, #1	Pt-Pd MEA, #2	PtCo-Pd MEA, #1	PtCo-Pd MEA, #2
Cell Temperature (°C)	79.5	64	66	62
Cathode Humidifier (°C)	74.5	64	64.5, Increased to 72 near end	62
Anode Humidifier (°C)	74	65	65.5, Increased to 70 near end	64
Cathode In-line Humidifier to cell (°C)	79.5	61, Increased to 90 near end	87, Decreased to 72 near end	75
Anode In-line Humidifier to cell (°C)	79.5	59, Increased to 80 near end	83, Decreased to 67 near end	73
H_2 flow rate (mL/min)	Increased from 46 to 168	73	73	73, Increased to 146 for several scans, then returned to 73
H_2 back pressure (psi)	Increased from 3.8 to 18.8	5	4.5	6
Air flow rate (mL/min)	Increased from 176 to 555	216	211	211
Air back pressure (psi)	Increased from 9.4 to 19.6	8	9	9

Table 2. General cell conditions, including temperature and gas flow rate and back pressure, for each of the four MEAs tested.

experiment. All temperatures were recorded. See Table 2 for the temperatures and flow rates of each of the MEAs tested.

Tested cells were conditioned according to the break-in period protocol developed by the USFCC [4]. Other load programs were performed on the cells including: square wave sequences (30 seconds at 0.6 V, 30 seconds at 0.96 V), constant current operation (at varying loads), and sequences where the cell was cycled between 0.5 V and 1.4 V for an hour and then bulk electrolysis was run at 1.4 V followed by 0.5 V. The high frequency impedance (HFI) of the MEAs was determined before and after cell conditioning and testing using A.C. impedance spectroscopy. Cyclic Voltammetry (CV) was performed on the cell using Corrware. The CV, bulk electrolysis and A.C. impedance were performed with a 1260A Impedance/Gain-Phase Analyzer and a 1287A Potentiostat (Solartron). See Table 3 for a description of the load sequences implemented with each MEA.

	Pt-Pd MEA, #1	Pt-Pd MEA, #2	PtCo-Pd MEA, #1	PtCo-Pd MEA, #2
Before Stage 1	N/A	N/A	Pol. curve	OCP for 1hr
Stage 1	0.6 V	0.6 V	0.6 V	0.6 V
Stage 2	0.7 V, 0.5 V for 9 cycles	0.7 V, 0.5 V for 9 cycles	0.7 V, 0.5 V for 9 cycles	0.7 V, 0.5 V for 9 cycles
After Stage 2	Pol. curve then 1 hr at OCP. Polarization curve then 1 hr at 1 amp, repeat	1 amp for 45 min, Pol. curve, 1 amp for 1 hr, 3 Pol. curves, 6 1-hr square wave sequences	2 Pol. curves — cycle down then up potential, constant current at 2 amps for 2.5 hr, 2 1-hr square wave sequences	1 hr at 1 amp, 2 hr at 3 amps, Pol. curve, bulk electrolysis at 0.5 V then 1.4 V for 3 cycles

Table 3. Electrical sequences implemented for each MEA, including voltage or current setting and length of time for each step. Polarization curve is abbreviated as Pol. curve. The square wave sequence consisted of 30 second steps at 0.6 V and 0.96 V.

Results

Cell parameters were monitored throughout the experiment and maintained at constant values within experimental constraints, with the goal of minimizing the active variables in the experiment. The first Pt-Pd MEA study was abbreviated due to poor electrical performance, operating at a maximum of 0.46 amps/cm^2 at 0.1 V, with the H_2 flow rate at 168 mL/min with a back pressure of 18.8 psi, air flow rate at 555 mL/min with a back pressure of 19.6 psi and the cell torqued to 110 psi. The HFI of the cell was 0.15 ohms, approximately an order of magnitude higher than expected. The second Pt-Pd MEA was then tested, yielding a much better performance. The second Pt-Pd MEA achieved a performance of 0.97 amps/cm^2 at 0.1 V, with the H_2 flow rate at 73 mL/min with a back pressure of 4.3 psi, and the air flow rate at 211 mL/min with a back pressure of 7.9 psi. The final HFI read 0.057 ohms. The first PtCo-Pd MEA showed lower performance as compared to the second Pt-Pd MEA. The first PtCo-Pd MEA was the first to exhibit negative response to the conditioning phase protocol. A polarization curve before conditioning demonstrates the cell performance to be operating at 0.90 amps/cm^2 at 0.1 V, while a polarization curve after the conditioning phase displayed cell performance to be 0.65 amps/cm^2 at 0.1 V with an HFI of 0.059 ohms. The second PtCo-Pd MEA demonstrated the expected performance increase during the conditioning phase. A polarization curve after stage 2 shows the cell performing at 0.90 amps/cm^2 at 0.1 V with an HFI of 0.058 ohms. Table 4 provides a summary of the electrochemical data for each MEA.

	Max Performance (amps/cm^2)	HFI, before test (ohms)	HFI, after test (ohms)
Pt-Pd MEA, #1	0.46	N/A	0.15
Pt-Pd MEA, #2	0.97	0.0768	0.057
PtCo-Pd MEA, #1	0.65	0.077	0.059
PtCo-Pd MEA, #2	0.90	N/A	0.056

Table 4. Electrochemical data for each MEA, including the maximum performance of each cell in amps/cm^2 (data shown is for 0.1 V) and the HFI before and after testing.

The fluorescence and transmission spectra were analyzed as a function of time. This research concentrates on the variations within the edge step of the spectra. This can lead to information concerning the behavior and environment of the PEFCs with regard to humidity and catalyst loss or modification (an increase in particle size for example). Both the fluorescence and transmission spectra demonstrate a decrease in edge step over time in general, but do have several spectra that do not fit this trend. During both of the Pt-Pd MEAs and both of the PtCo-Pd MEAs, several XAFS scans had to be discarded due to glitches in the XAFS spectra, which likely arose from condensed water bubbles in transition through the cell. The PtCo-Pd MEA tested at the Co-K edge consistently experienced glitches at about 8.3 keV while the glitches in the Pt-Pd MEAs were less localized, occurring just before and after the absorption edge and throughout the XAFS tail as well.

Discussion

The stable gas flow rates and cell and humidifier temperatures (Figure 3) indicate that observed catalyst loss and cell performance are not functions of these temperature parameters and thus more likely functions of either the electrical parameters in the conditioning phase or of the changing MEA environment with regard to water volume at the electrodes and in the PEM. Figure 4 shows fluorescence spectra from each of the four MEAs. A decrease of the EXAFS region indicates continual loss of fluorescing/absorbing material from the cathode, which is clearly present for the Pt-Pd MEAs as shown in Figure 4(a,b). Detailed scan to scan observations suggest that the water volume of the electrodes is dynamic, experiencing both increases and decreases as discussed later, but is consistent with a continual decrease in the fluorescence as a loss of Pt from the cathode. This continual decrease is not as clear in the spectra for the PtCo-Pd MEAs, suggesting that those MEAs are experiencing less catalyst loss. This is supported by examining the percent change in the edge step over time. The first Pt-Pd MEA ended at a fluorescence edge step that was 87.6% of the initial edge step and the second Pt-Pd MEA ended with a fluorescence edge step that was 79.0% of the original. Both PtCo-Pd MEAs increased, ending at 120.7% and 167.0% of the original, for the first and second respectively, which corroborates with the idea of low PtCo loss. The overall increase in the PtCo edge steps for each MEA arose from the water volume decreasing at the cathode during the 1.4 V bulk electrolysis steps. This trend is

present in both the Pt-L_3 edge spectra and the Co-K edge spectra. A look at the transmission spectra for all four MEAs shows a decrease in the height of the edge step. Because the decrease in the edge step is not present in the fluorescence spectra, the cause must be loss of material from the anode. As water has already been ruled unlikely due to the fluctuations observed, the decrease of the entire spectra suggests loss of Pt, Pd and/or carbon support. Loss of Pt would also be consistent with a decreasing edge step, however, as mentioned previously, the MEAs with PtCo cathodes actually showed increased Pt fluorescence, which is not consistent with Pt loss. The evidence thus suggests that the increased Pt transmission results from loss of Pd from the anode or support loss from either electrode.

The thrust of the analysis for this experiment examines the fluorescence and transmission edge steps, as they contain information regarding the changing MEA environment on a scan to scan basis. Figure 5 shows plots of the fluorescence and transmission edge steps plotted against time along with the potential and current for each of the MEAs tested. As described in Table 1, opposing changes in the edge step show correlation between the anode and cathode with respect to water activity. This correlation is clear in the second Pt-Pd MEA and in the PtCo-Pd MEAs but not in the first Pt-Pd MEA. The first Pt-Pd MEA demonstrated a high HFI and poor performance (Figure 6) compared to other MEAs as well, suggesting that it was running at a state of low relative humidity and was drying out, yielding the poor performance as protons are less able to traverse the PEM and reach the cathode. The second Pt-Pd MEA and both PtCo-Pd MEAs obtained low HFI readings, meaning there was low resistance in those MEAs, suggesting that the cells are operating at high relative humidity. A cell functioning at a high relative humidity, as long as flooding, which can be detrimental to cell performance, has not occurred, would be less affected by the production rate of water within the cell and less likely to show major fluctuation in water activity as a function of changing electrical parameters. This would result in an increased correlation between the fluorescence and transmission edge steps as the changing water level would be more closely related to humidity levels of the gas stream than of the amount of H_2O produced from the combination of protons and oxygen anions. The correlation between fluorescence and transmission edge steps along with the correlation between relative humidity and cell performance indicates that the conditioning phase has a component arising as a function of humidity, i.e., a period in which the cell becomes properly humidified so as to achieve optimized and stable performance.

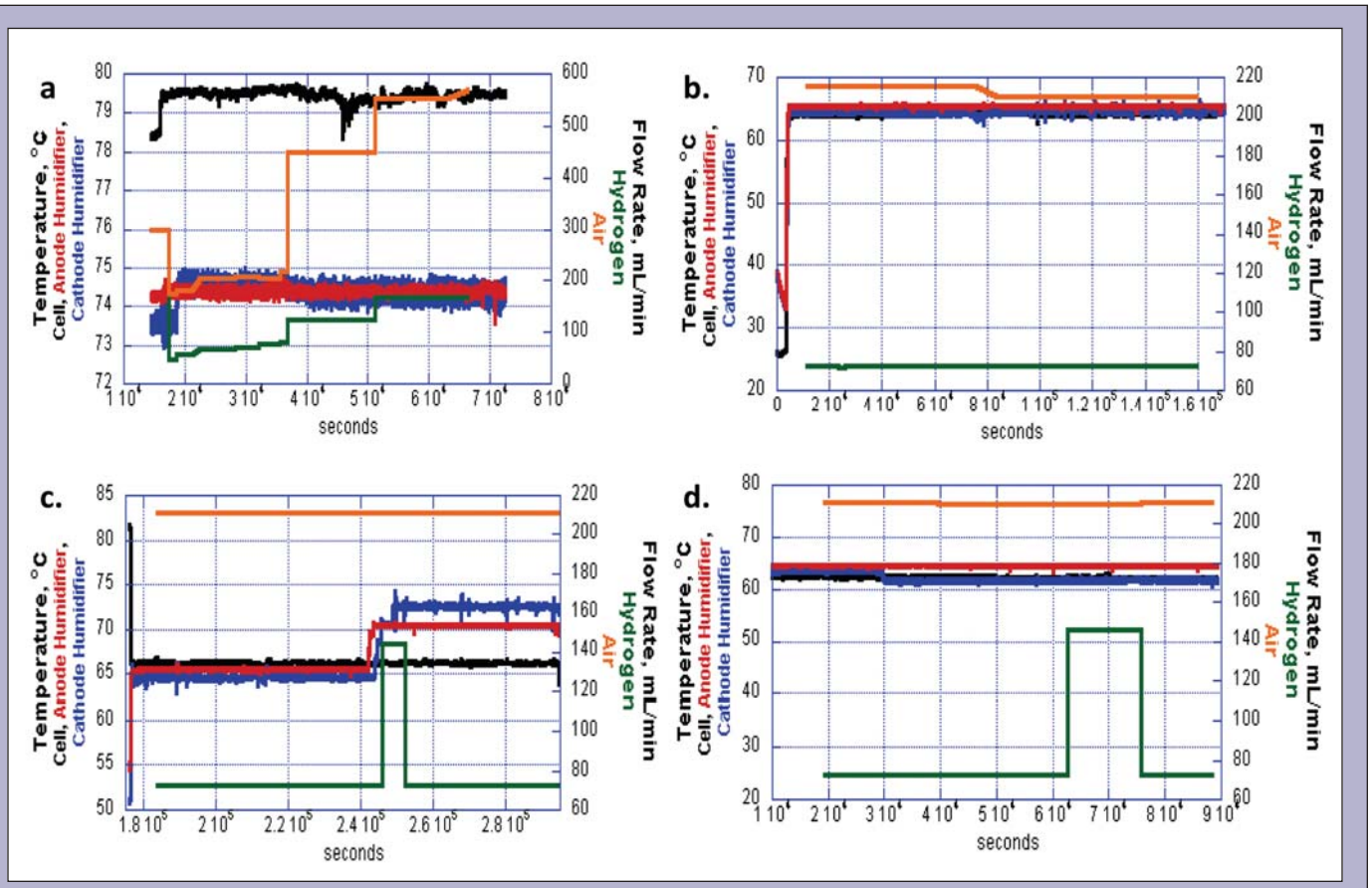

Figure 3. Gas flow rates and temperatures of the cell and humidifiers for **a.** the first Pt-Pd MEA, **b.** the second Pt-Pd MEA, **c.** the first PtCo-Pd MEA, **d.** the second PtCo-Pd MEA.

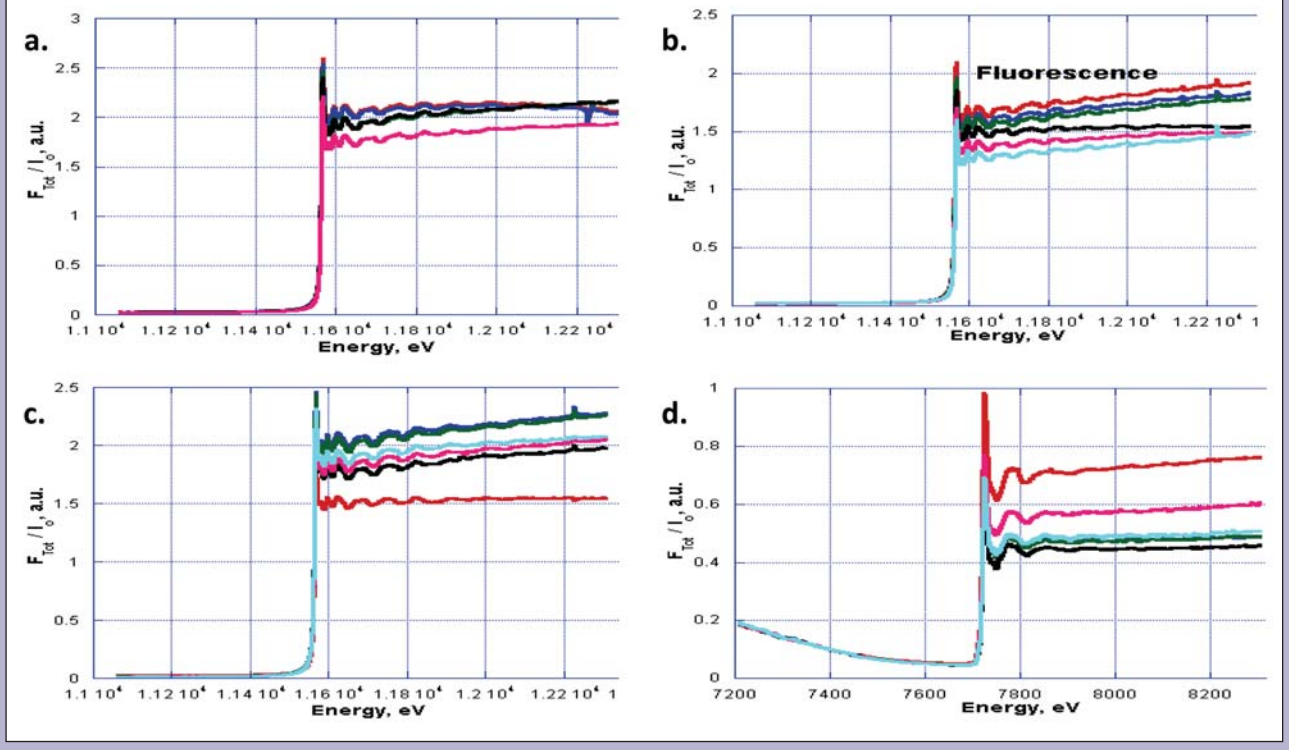

Figure 4. Fluorescence spectra over time for **a.** the first Pt-Pd MEA, **b.** the second Pt-Pd MEA, **c.** the first PtCo-Pd MEA, **d.** the second PtCo-Pd MEA. The color scheme in each graph is consistent with time (Red→Blue→Green→Black→Pink→Teal represents increasing time). The decrease in the EXAFS portion of the Pt-Pd MEA spectra indicates a continual loss in Pt. Note the lack of a downward trend with the PtCo spectra, suggesting less catalyst loss in the PtCo-Pd MEAs.

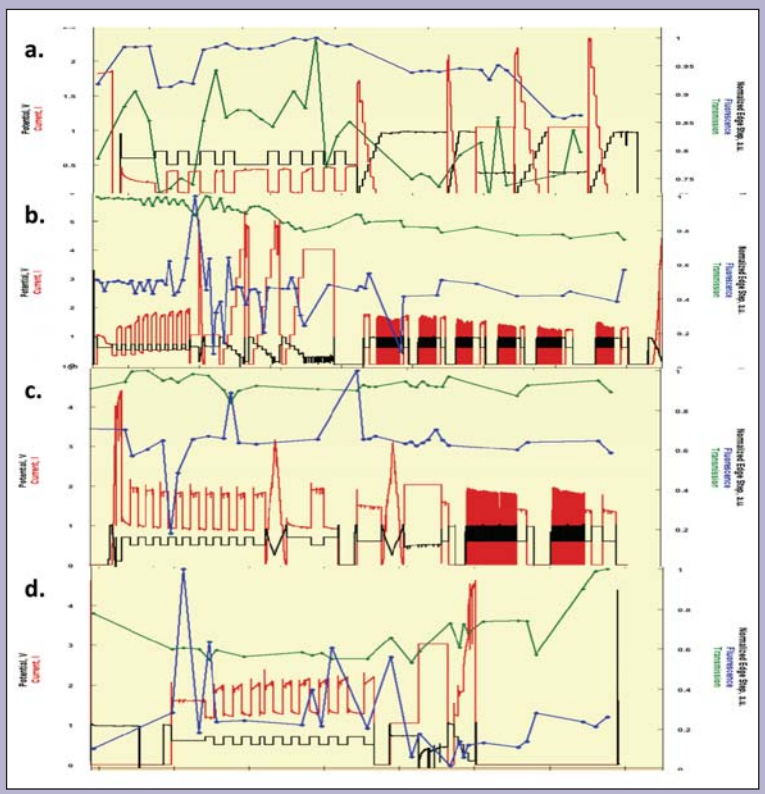

Figure 5. Fluorescence and transmission edge steps plotted against time along with the voltage and current sequences for **a.** the first Pt-Pd MEA, **b.** the second Pt-Pd MEA, **c.** the first PtCo-Pd MEA, **d.** the second PtCo-Pd MEA.

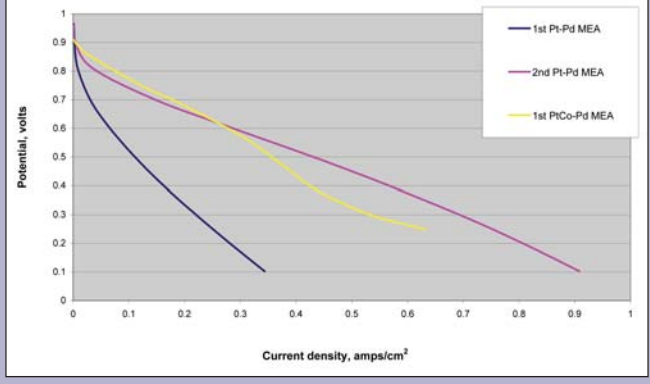

Figure 6. Polarization curves for the Pt-Pd MEAs and the first PtCo-Pd MEA run shortly after stage 2, highlighting the poor performance of the first Pt-Pd MEA.

Conclusion

The good correlation between the fluorescence and transmission edge steps in cells that performed well combined with the correlation between low HFI and improved cell performance gives preliminary evidence that cell conditioning is a function of humidity in the cell. This finding agrees with previous work stating the importance of good relative humidity on cell performance [7]. Note that these findings do not indicate that the more water the better, as flooding of the cell with too much water is a major issue, leading to poor reactant transport in the electrode layers and corrosion of the catalysts and supports within the fuel cell [7].

In testing both Pt-Pd MEAs and PtCo-Pd MEAs, the consistent decrease of the fluorescence edge step with the Pt-Pd MEAs as opposed to the rather consistent edge step with the PtCo-Pd MEAs suggests that PtCo/C may be a more durable electrocatalyst than Pt/C alone. However, the authors caution that a more thorough effort is required to fully substantiate this postulate.

There is undoubtedly more understanding of the conditioning phase that can be gained from further research. Further analysis of the EXAFS will give a better understanding of the atomic environment, including information on the coordination of Pt and interactions between the electrocatalyst and oxygen. Further experimentation should be completed to observe particle size during the conditioning phase, verifying whether loss of catalyst in the beam is actually catalyst getting washed from the electrode or if it is a function of catalyst rearrangement and growth in particle size.

Acknowledgements

I would like to thank Nancy Nega and Lou Harnisch, the Pre-Service Teacher program advisors, for their guidance throughout the summer. Also, I would like to thank Nadia Leyarovska, Nancy Kariuki and Xiaoping Wang for experimental help. This work was supported by the United States Department of Energy, Office of Science, Basic Energy Sciences.

References

[1] F. Urbani et al., "Effect of operative conditions on a PEFC stack performance," *International Journal of Hydrogen Energy*, vol. 33, pp. 3137–3141, June 2008.

[2] R. Borup, J. Meyers, B. Pivovar, Y.S. Kim, R. Mukundan, N. Garland, D. Myers, M. Wilson, F. Garzon, D. Wood, P. Zelenay, K. More, K. Stroh, T. Zawodzinski, J. Boncella, J.E. McGrath, M. Inaba, K. Miyatake, M. Hori, K. Ota, Z. Ogumi, S. Miyata, A. Nishikata, Z. Siroma, Y. Uchimoto, K. Yasuda, K.I. Kimijima and N. Iwashita, "Scientific aspects of polymer electrolyte fuel cell durability and degradation," *Chemical Reviews*, vol. 107, pp. 3904–3951, September 2007.

[3] H.A. Gasteiger, S.S. Kocha, B. Sompalli and F.T. Wagner, "Activity benchmarks and requirements for Pt, Pt-alloy, and non-Pt oxygen reduction catalysts for PEMFCs," *Applied Catalysis B-Environmental*, vol. 56, pp. 9–35, March 2005.

[4] "Single Cell Test Protocol," U.S. Fuel Cell Council's Single Cell Testing Task Force, Washington, DC, Report, July 13, 2006.

[5] A.E. Russell and A. Rose, "X-Ray absorption spectroscopy of low temperature fuel cell catalysts," *Chemical Reviews*, vol. 104, 4613–4635, August 2004.

[6] B. Ravel, Argonne National Laboratory, "Athena: background removal and normalization," 2005, http://cars9.uchicago.edu/xafs_school/APS_2005/CD/Docs/Athena/athena_bkg.html.

[7] W. Schmittinger and A. Vahidi, "A review of the main parameters influencing long-term performance and durability of PEM fuel cells," *Journal of Power Sources*, vol. 180, pp. 1–14, May 2008.